BBA - Molecular Basis of Disease 1865 (2019) 1298–1312

Contents lists available at ScienceDirect

BBA - Molecular Basis of Disease

journal homepage: www.elsevier.com/locate/bbadis

Adipocyte MTERF4 regulates non-shivering adaptive thermogenesis and sympathetic-dependent glucose homeostasis

Anna Castillo[a,1], Maria Vilà[a,1], Inés Pedriza[a], Rosario Pardo[a], Yolanda Cámara[b,c], Edgar Martín[a], Daniel Beiroa[d,e], Javier Torres-Torronteras[b,c], Marta Oteo[f], Miguel A. Morcillo[f], Ramon Martí[b,c], Rafael Simó[g,h], Rubén Nogueiras[d,e], Josep A. Villena[a,h,*]

[a] Laboratory of Metabolism and Obesity, Vall d'Hebron - Institut de Recerca, Universitat Autònoma de Barcelona, Barcelona, Spain
[b] Group of Mitochondrial and Neuromuscular Pathology, Vall d'Hebron - Institut de Recerca, Universitat Autònoma de Barcelona, Barcelona, Spain
[c] CIBERER, CIBER on Rare Diseases, Instituto de Salud Carlos III, Barcelona, Spain
[d] Department of Physiology, CIMUS, Universidad de Santiago de Compostela, Santiago de Compostela, Spain
[e] CIBEROBN, CIBER on Physiopathology of Obesity and Nutrition, Santiago de Compostela, Spain
[f] Centro de Investigaciones Energéticas, Medioambientales y Tecnológicas, Madrid, Spain
[g] Group of Diabetes and Metabolism, Vall d'Hebron - Institut de Recerca, Universitat Autònoma de Barcelona, Barcelona, Spain
[h] CIBERDEM, CIBER on Diabetes and Associated Metabolic Diseases, Instituto de Salud Carlos III, Barcelona, Spain

ARTICLE INFO

Keywords:
Mitochondrial transcription termination factor 4
Mitochondrial biogenesis
Brown adipose tissue
Non-shivering adaptive thermogenesis
β_3-adrenoreceptor agonist
Glucose homeostasis

ABSTRACT

In humans, low brown adipose tissue (BAT) mass and activity have been associated with increased adiposity and fasting glucose levels, suggesting that defective BAT-dependent thermogenesis could contribute to the development of obesity and/or type 2 diabetes. The thermogenic function of BAT relies on a vast network of mitochondria exclusively equipped with UCP1. Mitochondrial biogenesis is exquisitely regulated by a well-defined network of transcription factors that coordinate the expression of nuclear genes required for the formation of functional mitochondria. However, less is known about the mitochondrial factors that control the expression of the genes encoded by the mitochondrial genome. Here, we have studied the role of mitochondrial transcription termination factor-4 (MTERF4) in BAT by using a new mouse model devoid of MTERF4 specifically in adipocytes (MTERF4-FAT-KO mice). Lack of MTERF4 in BAT leads to reduced OxPhos mitochondrial protein levels and impaired assembly of OxPhos complexes I, III and IV due to deficient translation of mtDNA-encoded proteins. As a result, brown adipocytes lacking MTERF4 exhibit impaired respiratory capacity. MTERF4-FAT-KO mice show a blunted thermogenic response and are unable to maintain body temperature when exposed to cold. Despite impaired BAT function, MTERF4-FAT-KO mice do not develop obesity or insulin resistance. Still, MTERF4-FAT-KO mice became resistant to the insulin-sensitizing effects of β_3-specific adrenergic receptor agonists. Our results demonstrate that MTERF4 regulates mitochondrial protein translation and is essential for proper BAT thermogenic activity. Our study also supports the notion that pharmacological activation of BAT is a plausible therapeutic target for the treatment of insulin resistance.

1. Introduction

Brown adipose tissue (BAT) is specialized in the generation of heat to maintain body temperature in response to cold through a process known as non-shivering adaptive thermogenesis [1]. The thermogenic activity of BAT depends on the exclusive expression in brown adipocytes of UCP1, a protein located in the inner membrane of mitochondria that functions as a proton channel and uncouples substrate oxidation (i.e. fatty acids and glucose) from the synthesis of ATP. As a result, the energy accumulated as an electrochemical gradient generated by the respiratory chain is dissipated as heat [2]. In addition to brown adipocytes located in BAT depots, brown-like adipocytes can be also found interspersed within white adipose tissue (WAT) [3,4]. These so-called "brite" or "beige" adipocytes, which are ontogenically distinct from "classical" brown adipocytes of BAT [5], express UCP1 in sufficient amounts to become thermogenically competent [6]. Increased occurrence and thermogenic activity of both brown and beige adipocytes have been shown to protect against obesity and metabolic disease in a

* Corresponding author at: Laboratory of Metabolism and Obesity, Vall d'Hebron-Institut de Recerca, Passeig Vall d'Hebron, 119-129, Barcelona 08035, Spain.
E-mail address: josep.villena@vhir.org (J.A. Villena).
[1] These authors contributed equally to this work.

https://doi.org/10.1016/j.bbadis.2019.01.025
Received 24 September 2018; Received in revised form 15 January 2019; Accepted 23 January 2019
Available online 26 January 2019
0925-4439/

variety of rodent models (reviewed in [7]). Interestingly, low BAT mass and activity in adult humans have been associated with increased adiposity and high fasting glucose levels, suggesting that defective BAT-dependent thermogenesis could contribute to the development of obesity and/or type 2 diabetes [8,9]. Given its capacity to influence whole body energy and glucose homeostasis, BAT is nowadays viewed as a promising target for the treatment of metabolic diseases.

Unlike white adipocytes, which show low mitochondrial mass and limited oxidative capacity, the thermogenic function of brown and beige adipocytes relies on the presence of a vast mitochondrial network. Although subjected to dynamic changes in response to nutritional and environmental cues, the mitochondrial population of brown adipocytes is acquired during the maturation of BAT at late fetal stages in the absence of thermogenic stress or as the result of the differentiation of precursor cells in response to thermogenic stimuli [10,11]. The generation of new mitochondria is a complex process that requires the coordinated expression of hundred of genes encoded by two compartmentalized genomes: the nuclear (nDNA) and the mitochondrial (mtDNA) genomes. Mitochondrial biogenesis in BAT has been shown to be tightly controlled at the transcriptional level by set of key transcription factors that include NRF-2/GABP [12], ERRα/γ [13,14] and the transcriptional co-activators PGC-1α and β [10,15,16], all of which directly control the expression of nDNA-encoded mitochondrial genes. Less is known about how the expression of mtDNA-encoded genes is controlled in brown adipocytes. Mitochondrial transcription factors TFAM and TFB2M are known to coordinate the transcription of the mtDNA genes in several cell types and tissues (reviewed in [17]), but detailed information about their specific functional relevance in BAT is still missing.

The MTERF (mitochondrial transcription termination factor) family of proteins, that include MTERF1, 2, 3 and 4, constitute, from the functional point of view, a heterogeneous group of mitochondrial factors whose function in the control of the expression of mtDNA-encoded genes remains to be fully elucidated. MTERF1, the founding member of the family, was described as a terminator of the transcription of the mtDNA H-strand [18]. However, more recent studies suggest that MTERF1 only acts as a partial terminator of H-strand transcription whereas it completely terminates L-strand transcription as a way to prevent the antisense transcription of the ribosomal RNA genes [18]. The function of MTERF2 remains completely unknown, although it has been suggested that it could work as a positive regulator of mtDNA transcription [19]. Contrarily, MTERF3 has been described as a repressor of mtDNA transcription [20]. Still, others studies have suggested that MTERF3 could be involved in the control of mitochondrial protein translation by participating in the assembly of the large mitochondrial ribosomal subunit through its interaction with the 16S rRNA [21]. Contrarily to MTERF2 and 3, no direct role in mtDNA transcription or replication has been attributed to MTERF4. Instead, the most recent studies suggest that MTERF4 participates in the assembly of mitochondrial ribosomes by partnering with the mitochondrial methyltransferase NSUN4 and by this means it regulates mitochondrial protein translation [22]. Global loss of MTERF4-NSUN4 complexes leads to embryonic lethality, whereas heart-specific deletion of either protein leads to reduced assembly of mitochondrial ribosomes and impaired cardiac mitochondrial function that results in premature death [22,23]. Still, the functional relevance of MTERF4 in other tissues, such as BAT, where mitochondria are highly abundant, remains to be explored.

2. Material and methods

2.1. Generation of adipose-specific Mterf4 knockout mice

Adipose-specific *Mterf4* knockout mice, from now on referred as MTERF4-FAT-KO, were generated by crossing mice carrying loxP sites flanking exon 2 of the *Mterf4* gene (*Mterf4*$^{flox/flox}$) [22] with transgenic mice that overexpress Cre recombinase under the adipocyte-specific promoter of adiponectin (AdipoQ-Cre) (The Jackson Laboratory) [24]. For all our experiments, animals were housed in a temperature-controlled environment at 21 °C, subjected to a 12/12 h light/dark cycle and fed a standard diet (2018 Tecklad Global 18% Protein Rodent Diet, 18% Kcal from fat, Harlan Laboratories, USA) unless otherwise stated. Only males were used in this study.

All procedures involving animal experimentation were approved by the Animal Experimentation and Ethics Committee of the Vall d'Hebron Research Institute (ID 66/17 CEEA) and were carried out according to the EU Directive 2010/63/EU for animal experimentation.

2.2. Acute cold exposure

For the acute cold exposure experiments, 10-week old MTERF4-FAT-KO male mice fed a standard diet and their wild type (Wt) littermates were used. Animals were first individually caged with free access to water and food (standard diet) but no bedding. Basal core body temperature was determined with a rectal probe and then mice were immediately transferred to a room set at 4 °C. Body temperature was regularly measured every hour for a period of 5 h. A group of control Wt and MTERF4-FAT-KO mice was maintained in parallel at room temperature (21 °C) for the entire duration of the experiment. Afterwards, mice were euthanized by cervical dislocation, BAT and WAT depots isolated, snap frozen in liquid nitrogen and stored at −80 °C until further analysis. Additionally, a small piece of BAT was kept for histological analysis.

2.3. Whole body composition and indirect calorimetry

Whole-body composition was measured using nuclear magnetic resonance (NMR) imaging (Whole Body Composition Analyzer; EchoMRI, Houston, TX, USA). Energy expenditure and locomotor activity was assessed using a TSE LabMaster modular research platform (TSE Systems, Germany), as previously described [25]. Briefly, 16-week old male mice fed a standard diet were first acclimated to the test chambers during 48 h prior to the collection of O_2 consumption, CO_2 production and ambulatory activity data, which were recorded for an additional period of 48 h. The data collected were used to determine energy expenditure and locomotor activity.

To evaluate the thermogenic function of BAT in MTERF4-FAT-KO mice, oxygen consumption was determined immediately after an acute injection of the β_3-adrenoreceptor agonist CL316,243. For this, Wt and MTERF4-FAT-KO mice were placed in and acclimated to the calorimetric system cages for 48 h and then a single dose (1 mg/Kg) of CL316,243 was intraperitoneally administered. Oxygen consumption was measured 2 h before and 2 h after the administration of the β_3-receptor agonist.

2.4. Thermal imaging

Skin temperature of the interscapular region was recorded with an infrared thermal imaging camera (T420 Compact-Infrared-Thermal-Imaging-Camera, FLIR Systems) in 9-week old male mice fed a standard diet. For this, the day prior to the acquisition of thermal images, the interscapular region of mice was depilated. On the next day, 5–6 dorsal images of each mouse were taken and analyzed with the FLIR QuickReport 2.1 SP2 software. Specifically, for each image, a region of interest (ROI) covering the interscapular region was drawn and the maximal temperature within this region was determined. The maximal temperature of the interscapular region of each mouse was calculated by averaging the maximal temperature obtained for all the images taken from every mouse.

2.5. Gene expression

Gene expression was analyzed as previously described [26]. Briefly, total RNA was first isolated from tissues with Trizol (Invitrogen) and cDNA was then synthesized from 400 ng of RNA using SuperScript II reverse transcriptase (Invitrogen) and oligo dT primers. Gene expression was assessed by quantitative PCR using gene-specific primers (Supplementary Table 1) and SYBR green dye. Forty amplification cycles were carried out at the following conditions: denaturing 95 °C 20s, annealing 60 °C 20s, extension 72 °C 34s. Relative gene expression was calculated according to the $2^{-\Delta\Delta Ct}$ threshold method using cyclophilin A as reference gene.

2.6. Western blot

Protein from WAT, BAT and skeletal muscle was prepared in extraction buffer (50 mM Tris pH = 8.0, 150 mM NaCl, 0.5% Sodium deoxycolate, 1% SDS, 1% Triton X-100) supplemented with protease inhibitors. Thirty to fifty microgram of protein extract were subjected to electrophoresis in a 10% or 12% SDS/PAGE and transferred to a PVDF membrane. Immunodetection was performed with specific antibodies to detect UCP1 (uncoupling protein 1), COXI (cytochrome *c* oxidase subunit I), NDUFB9 (NADH:ubiquinone oxidoreductase subunit B9), ACO2 (aconitase 2), SDHB (succinate dehydrogenase subunit B) (Abcam, UK), COXIV (cytochrome *c* oxidase subunit IV) and α-tubulin (Merck Millipore, USA).

2.7. Histology

Interscapular BAT was fixed overnight in 4% formaldehyde. After dehydration in a series of ethanol solutions of increasing concentration, the tissue was embedded in paraffin for subsequent sectioning. Tissue sections (5–8 μm) were stained with hematoxylin/eosin and images were taken using a BX61 Olympus microscope.

2.8. Transmission electron microscopy

BAT of 12-week old MTERF4-FAT-KO male mice and their Wt littermates was dissected, cut into small pieces of 1–2 mm^3 and fixed in 2.5% glutaraldehyde/2% paraformaldehyde in 0.1 M phosphate buffer (pH = 7.4). After washing, samples were postfixed with 1% OsO_4 in cacodylate buffer. Samples were dehydrated in graded acetone series and embedded in epoxy resin. Ultrathin sections were mounted on copper grids, contrasted with uranyl acetate/lead citrate and examined in a Jeol JEM-1400 transmission electron microscope equipped with a Gatan Ultrascan ES1000 CCD camera.

2.9. Enzymatic activity of mitochondrial respiratory chain complexes

To determine the activity of mitochondrial respiratory chain complexes, mitochondria were first purified by differential centrifugation. Interscapular, axillar, and cervical BAT depots from 10- to 12-week old MTERF4-FAT-KO mice and Wt littermates fed a standard diet were isolated, pooled and homogenized in a Potter-Elvehjem tissue homogenizer in homogenization buffer (0.25 M sucrose, 5 mM TES, 0.2 mM EGTA and 0.5% fatty acid-free BSA, pH = 7.2). Samples were then centrifuged at 8500*g* for 10 min, the supernatant discarded and the mitochondria-containing pellet resuspended in homogenization buffer. Samples were then centrifuged at 800 *g* for 10 min to pellet nuclei and cell debris. Next, the supernatant was centrifuged at 8500*g* for 10 min to recover the mitochondrial fraction. The pelleted mitochondria were washed once in KCl/TES buffer (100 mM KCl/20 mM TES, pH = 7.2) and finally resuspended in the same buffer. Mitochondria were subjected to three cycles of freezing and thawing to disrupt membrane integrity and then protein content was measured by using the bicinchoninic acid method (Pierce, IL, USA). Eighty to one hundred and sixty microgram of protein were used to measure respiratory chain complex activity by spectrophotometric methods as follows:

NADH-ubiquinone oxidoreductase (complex I)

Reaction mix was prepared by adding protein extracts and 10 μl of 10 mM NADH to 950 μl of reaction buffer (50 mM KCl, 1 mM EDTA, 10 mM Tris-HCl, 2 mM KCN, 300 nM antimycin, pH = 7.4). After 1 min, 5 μl of 10 mM decylubiquinone were added to start the reaction. The oxidation rate of NADH was measured on a spectrophotometer at 340 nm during 2 min at 30 °C. Then, rotenone was added to stop the NADH-ubiquinone oxidoreductase specific activity. The rotenone-insensitive rate was measured for 10 min and subtracted from the rate of NADH disappearance.

Succinate dehydrogenase (complex II)

Reaction was carried at 30 °C in 950 μl of buffer (50 mM K-phosphate, 0.1 mM EDTA, 0.01% TritonX, 2 mM KCN, 300 nM antimycin, 10 μM rotenone). Fifty microliter of mitochondrial protein extract and 20 μl of 1 mM of succinate were added and 5 min later the reaction was started by the addition of 40 μM dichloroindophenol and 20 μM decylubiquinone. Succinate dehydrogenase activity was monitored at 600 nm for 3 min. Succinate dehydrogenase rate was calculated after subtracting non-specific enzymatic activity, which was determined by the addition of 0.5 mM of thenoyltrifluoroacetone.

Succinate dehydrogenase + ubiquinone-cytochrome *c* reductase (complex II + III)

Coupled succinate dehydrogenase and ubiquinone-cytochrome *c* reductase activities were measured as the rate of cytochrome *c* reduction with succinate as the electron donor. Sixty microliter of mitochondrial extract were first incubated in reaction buffer (50 mM K-phosphate, 0.1 mM EDTA, 2 mM KCN, 10 μM rotenone, 20 mM succinate, pH = 7.4) during 5 min. Then, the reaction was initiated by adding 50 μM of oxidized cytochrome *c* and monitored at 550 nm during 3 min. Non-enzymatic rates were calculated after adding 0.2 μg of complex III inhibitor myxothyazol.

Cytochrome c oxidase (complex IV)

Cytochrome c oxidase activity was determined by using a cytochrome *c* oxidase assay kit (Sigma, St. Louis, USA).

2.10. Oxygen consumption in isolated brown adipocytes

The interscapular, cervical and axillar BAT depots from 2 to 3 Wt or MTERF4-FAT-KO mice fed a standard diet were carefully dissected, pulled and washed with DMEM:F12 media. BAT was then finely minced with scissors and subjected to collagenase digestion for 30–40 min at 37 °C in digestion buffer (100 mM Hepes, pH = 7.4, 123 mM NaCl, 5 mM KCl, 1.3 mM CaCl2, 5 mM glucose, 1.5% bovine serum albumin and 1 mg/ml of Collagenase A). After the digestion process was completed, the cell suspension was filtered through a 70 μm nylon cell strainer to remove undigested tissue fragments and the cell suspension was kept still for 20 min to allow mature brown adipocytes float to the top. Floating brown adipocytes were recovered, resuspended in DMEM:F12 media, counted and immediately used for respiration studies. Basal and norepinephrine-stimulated oxygen consumption was measured with a Clark-type oxygen electrode (Hansatech Instruments Ltd.). In each experiment, 5×10^4 cells were added to the oxygen electrode chamber containing respiration media (DMEM:F12, 5% CO_2, pH = 7.4) and subjected to very mild magnetic stirring (100 rpm). Basal respiration was measured for 2–4 min. Then, 1 mM norepinephrine was added and oxygen consumption monitored for an additional period of 3–5 min. Background was estimated as the oxygen decrease measured over 1 min after the inhibition of mitochondrial respiration with 1 mM KCN. Data shown are the average of 4 independent experiments with 2–3 respiration measurements per experiment.

2.11. In vivo lipolysis assay

To determine the effect that lack of MTERF4 has on lipolysis, levels of circulating free-fatty acids were determined in serum of Wt and MTERF4-FAT-KO mice at time 0 (basal) and 15 min after an intraperitoneal injection of isoproterenol (10 mg/kg). Non-esterified fatty acids were measured with the NEFA-C kit (Wako Chemicals GmbH, Germany).

2.12. Glucose and insulin tolerance tests

Glucose tolerance tests were performed on 12 h fasted mice. After an intraperitoneal injection of glucose (2 g/Kg body weight), blood glucose was measured at 0, 30, 60, 90 and 120 min. For insulin tolerance tests, mice were fasted for 5 h and then blood glucose was measured at 0, 30, 60, 90 and 120 min following an intraperitoneal injection of insulin (0.75–0.85 U/Kg of body weight). Glucose levels were measured in blood using an ELITE glucometer (Bayer, Spain).

2.13. Positron emission tomography

PET imaging was performed on 15-week old Wt and MTERF4-FAT-KO mice fed a standard diet using a small-animal Raytest ClearPET™ scanner. [^{18}F]-fluorodeoxyglucose ([^{18}F]-FDG) uptake was determined in the same animal under basal conditions (saline) or after stimulation with 1 mg/Kg of CL316,243. Mice were fasted overnight and 1 h after the intraperitoneal administration of CL316,243 or saline, 7–9 MBq [^{18}F]-FDG were injected into the tail vein. During the uptake period, the mice were conscious. PET studies (energy window 250–750 keV and 16 min static acquisition) were performed at 1 h post-injection in mice under 2% isoflurane anesthesia.

A calibration factor predetermined by scanning a cylindrical phantom containing a known activity of ^{18}F was used to convert counts per pixel/sec to kBq/cm^3. Regions of interest (ROIs) were manually drawn on sagittal PET images for interscapular regions in saline-treated mice or defined by isocontour (applying a threshold of 20% relative to SUV_{max}) in mice upon ß$_3$-adrenergic stimulation. ROIs were placed in the right lung as background activity. From each ROI, SUV_{mean} (mean standardized uptake value), SUV_{max} (single voxel with maximum value) and BAT-to-background ratios were measured for PET quantification. Images were analyzed using the image analysis software AMIDE [27].

2.14. Blue native polyacrylamide gel electrophoresis

Mitochondria from BAT of Wt and MTERF4-FAT-KO mice fed a standard diet were isolated as indicated (see section 2.9). Mitochondria were resuspended in 1.75 M Aminocaproic acid, 75 mM BisTris (pH = 7.0), 2 mM EDTA to a final concentration of 1–3 mg/ml and solubilized with 1% lauryl maltoside for 15 min on ice. After solubilization, samples were centrifuged at 4 °C and 20,000 g for 20 min and supernatants were collected and supplemented with Coomassie Brilliant Blue-G up to 0.25% (dissolved in 750 mM amminocaproic acid). Thirty microgram of solubilized protein was loaded onto 4–20% Bis-Tris NuPAGE pre-cast polyacrylamide gradient gels (Invitrogen) and resolved by blue native electrophoresis (BN-PAGE) [28]. Resolved BN-PAGE gels were either fixed and stained with 0.1% Coomassie Brilliant Blue-R or wet-transferred to PVDF membranes. Western blotting was performed using primary antibodies raised against Complex I 39 kDa subunit, Complex II 70 kDa subunit, Complex III core 2 subunit, and Complex IV subunit I. Peroxidase-conjugated anti-mouse immunoglobulins were used as secondary antibodies. The signal was detected after incubation with Immobilon Western Chemiluminescent HRP Substrate (Millipore).

2.15. In organello translation

In organello translation assay was performed as previously described with minor modifications [22]. A volume of mitochondrial suspension containing 0.3 mg of BAT mitochondria was centrifuged for 2 min at 10,000 g and 4 °C. The mitochondrial pellet was washed once with 1 ml of translation buffer and centrifuged for 2 min at 10,000 g and 4 °C. Then, the mitochondria were incubated at 37 °C with gentle rotation for 5 min in 300 µl of translation mix containing 60 µg/ml of all amino acids except methionine (0.1 M manitol, 10 mM sodium succinate, 80 mM potassium chloride, 5 mM magnesium chloride, potassium phosphate monobasic 1 mM, 60 µg/ml of each amino acid, 5 mM ATP, 20 mM GTP, 6 mM phosphocreatine, 60 µg/ml creatine kinase, and 2 m5 M HEPES, pH = 7.4). Easy Tag Express35S Protein labeling mix, a mix of [^{35}S]-Methionine and [^{35}S]-Cysteine (Perkin Elmer), was added to a final concentration of 0.35 mCi/ml. After 1 h of incubation with gentle rotation at 37 °C, mitochondria were washed in translation buffer and resuspended in a conventional SDS-PAGE loading buffer. Translation products were separated by SDS-PAGE and analyzed by autoradiography. Coomassie-staining of the SDS-PAGE gels was used as loading control.

2.16. Statistical analysis

Data are presented as mean ± SEM. Statistical significance was assessed using an unpaired Student's *t*-test or an analysis of the variance (ANOVA) followed by Tukey post hoc test.

3. Results

3.1. Mice lacking MTERF4 in adipose tissues show a selective reduction of OxPhos proteins

To study the role of MTERF4 in adipose tissues, we generated an adipose-specific *Mterf4* knockout mouse model by crossing *Mterf4*$^{flox/flox}$ mice with transgenic mice that express Cre recombinase under the control of the adiponectin promoter. Consistent with the specificity of the adiponectin promoter, MTERF4-FAT-KO mice exhibited a significant decrease in the *Mterf4* mRNA levels in WAT and BAT, but not in other tissues (Fig. 1A). The levels of mtDNA-encoded OxPhos proteins, like COXI, were severely decreased, but still detectable, in WAT and BAT, but they were not affected by the lack of MTERF4 in skeletal muscle (Fig. 1B–C). Interestingly, we observed that the expression of nuclear-encoded OxPhos subunits followed an unexpected and variable pattern. Whereas the levels of OxPhos proteins belonging to Complex II (i.e. SDHB), the only complex whose subunits are all encoded by the nuclear genome, remained unchanged in adipose tissues or even slightly increased in WAT, the levels of nuclear-encoded proteins belonging to OxPhos Complexes I (NDUFB9) and IV (COXIV) where dramatically decreased in both WAT and BAT (Fig. 1B–C). Considering the relevant role proposed for brown adipocytes in the control of energy and glucose homeostasis [7] and previous studies from our laboratory indicating that reduced mitochondrial biogenesis in WAT does not affect body weight or insulin sensitivity [29], we decided to pursue our study exclusively on BAT.

3.2. Impaired mtDNA-encoded protein translation and OxPhos complex assembly in MTERF4-FAT-KO mice

To investigate if reduced levels of mtDNA-encoded proteins in MTERF4-FAT-KO was due to impaired de novo mitochondrial protein synthesis, we performed *in organello* translation studies in isolated mitochondria from BAT of Wt and MTERF4-FAT-KO littermates. As shown in Fig. 2, protein translation was severely decreased in mitochondria isolated from BAT of mice lacking MTERF4.

To further study the reason by which the levels of OxPhos subunits belonging to complexes that contain mtDNA-encoded subunits were decreased even if such subunits were encoded by the nuclear genome, we analyzed the assembly of OxPhos complexes by BN-PAGE (Fig. 3A).

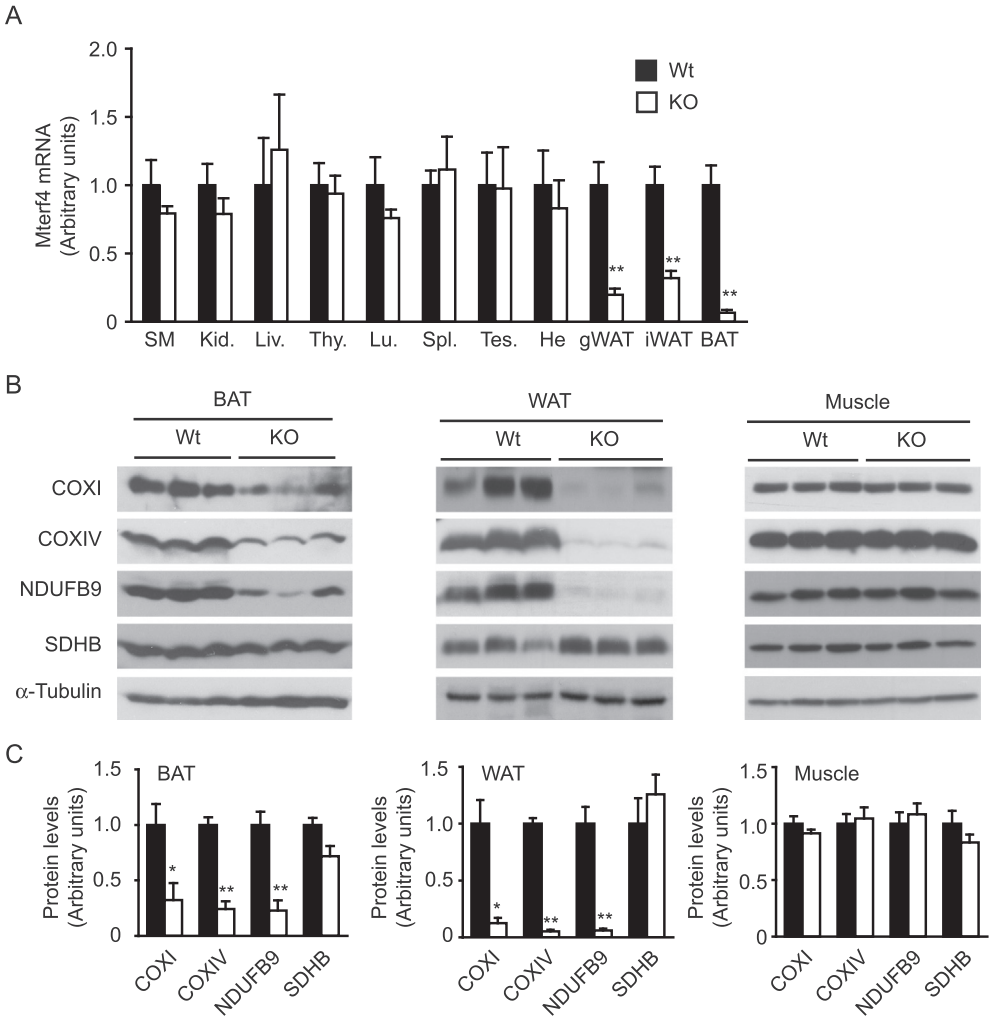

Fig. 1. Lack of MTERF4 specifically in adipocytes leads to reduced levels of OxPhos proteins in adipose tissues. (A) mRNA expression in tissues of 15-week old Wt and MTERF4-FAT-KO male mice fed a standard diet was assessed by real-time quantitative PCR. (SM, skeletal muscle; Kid., Kidney; Liv., Liver; Thy., Thymus; Lu., Lung; Spl., Spleen; Tes., Testis; He., Heart; gWAT, Gonadal WAT; iWAT, Inguinal WAT). Results are expressed as mean ± SEM ($n = 5$ animals/group; $^{**}P \leq 0.01$. (B) Levels of representative OxPhos proteins were detected by western blot in protein extracts from BAT, WAT and skeletal muscle. (C) Densitometric quantification of western blots ($n = 3$ mice/group; $^{*}P \leq 0.05$. $^{**}P \leq 0.01$).

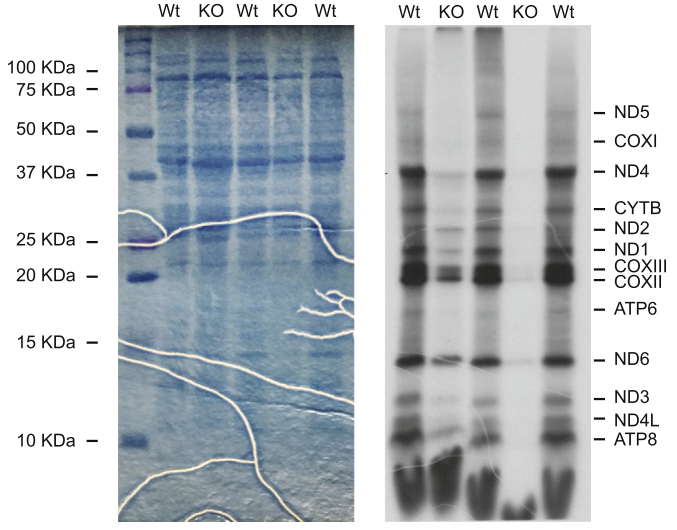

Fig. 2. Impaired translation of mtDNA-encoded genes in BAT of mice lacking MTERF4. De novo mitochondrial translation was analyzed in isolated mitochondria from BAT of Wt and MTERF4-FAT-KO male mice fed a standard diet ($n = 2$–3 mice/group). Coomassie blue staining of the polyacrylamide gels (left panel) is shown to demonstrate equal protein loading of all samples.

Levels of the assembled OxPhos complexes I, III and IV, which contain both mtDNA- and nDNA-encoded subunits, were decreased by 40–60% in mitochondria from BAT of MTERF4-FAT-KO mice (Fig. 3). Contrarily, the levels of assembled complex II, which has all constituent subunits encoded by the nDNA, were maintained in BAT of mice lacking MTERF4 when compared to their Wt littermates.

To determine how lack of MTERF4 and the consequent decrease in the translation of mtDNA-encoded genes affected mitochondrial biogenesis, we first estimated mitochondrial mass by measuring mtDNA content in BAT. As shown in Fig. 4A, a non-statistically significant mild increase in mtDNA content was observed in BAT of MTERF4-FAT-KO mice. Furthermore, ultrastructural analysis of BAT revealed that brown adipocytes from MTERF4-FAT-KO were bigger and accumulated more triglycerides in large lipid droplets than their Wt littermates (Fig. 4B). Remarkably, mitochondria from MTERF4-FAT-KO mice looked very similar in size and shape to the ones from Wt mice, but they appeared to have shorter cristae (Fig. 4B). Moreover, despite impaired mitochondrial protein translation and assembly of OxPhos complexes, no compensatory transcriptional response in BAT of MTERF4-FAT-KO mice was observed for nuclear or mitochondrial genes encoding for mitochondrial OxPhos proteins (Fig. 4C, left panel). Accordingly, no change in the expression of major transcriptional regulators of mitochondrial biogenesis was observed in BAT of mice lacking MTERF4 (Fig. 4C, right panel).

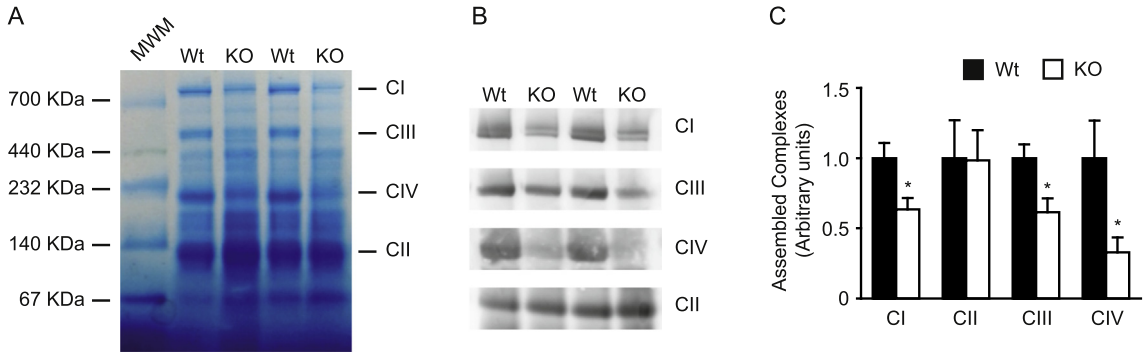

Fig. 3. Reduced OxPhos complex assembly in BAT of MTERF4-FAT-KO mice. (A) Blue native polyacrylamide gel electrophoresis of isolated mitochondria from BAT of Wt and MTERF4-KO mice fed a standard diet was carried out to analyze the levels of assembled OxPhos complexes. (B) Immunodetection of each complex was achieved by using antibodies raised against Complex I 39 kDa subunit, Complex II 70 kDa subunit, Complex III core 2 subunit, and Complex IV subunit I. (C) Densitometric quantification of assembled complexes detected with specific antibodies in BN-PAGE (n = 6 mice/group; $^*P \leq 0.05$).

3.3. Mice lacking MTERF4 exhibit reduced respiratory chain complex activity and impaired brown adipocyte respiration

To determine how lack of MTERF4 affected the oxidative capacity of BAT, we first isolated mitochondria from Wt and MTERF4-FAT-KO mice and determined the activity of the respiratory chain complexes I to IV (Fig. 5A). Consistent with the reduction in the levels of assembled complexes I and IV, NADH-ubiquinone oxidoreductase (Complex I) and cytochrome *c* oxidase (Complex IV) activities were decreased around 50% in BAT of MTERF4-FAT-KO mice. Contrarily, succinate dehydrogenase activity (Complex II) was found significantly increased in mitochondria of MTERF4-FAT-KO mice, whereas coupled activity of complexes II + III was not significantly altered (Fig. 5A).

To gain insight into how impaired OxPhos complex function affected the respiratory capacity of brown adipocytes, we isolated mature brown adipocytes from BAT of Wt and MTERF4-FAT-KO mice and determined oxygen consumption under basal conditions and after stimulation with norepinephrine. As shown in Fig. 5B, brown adipocytes

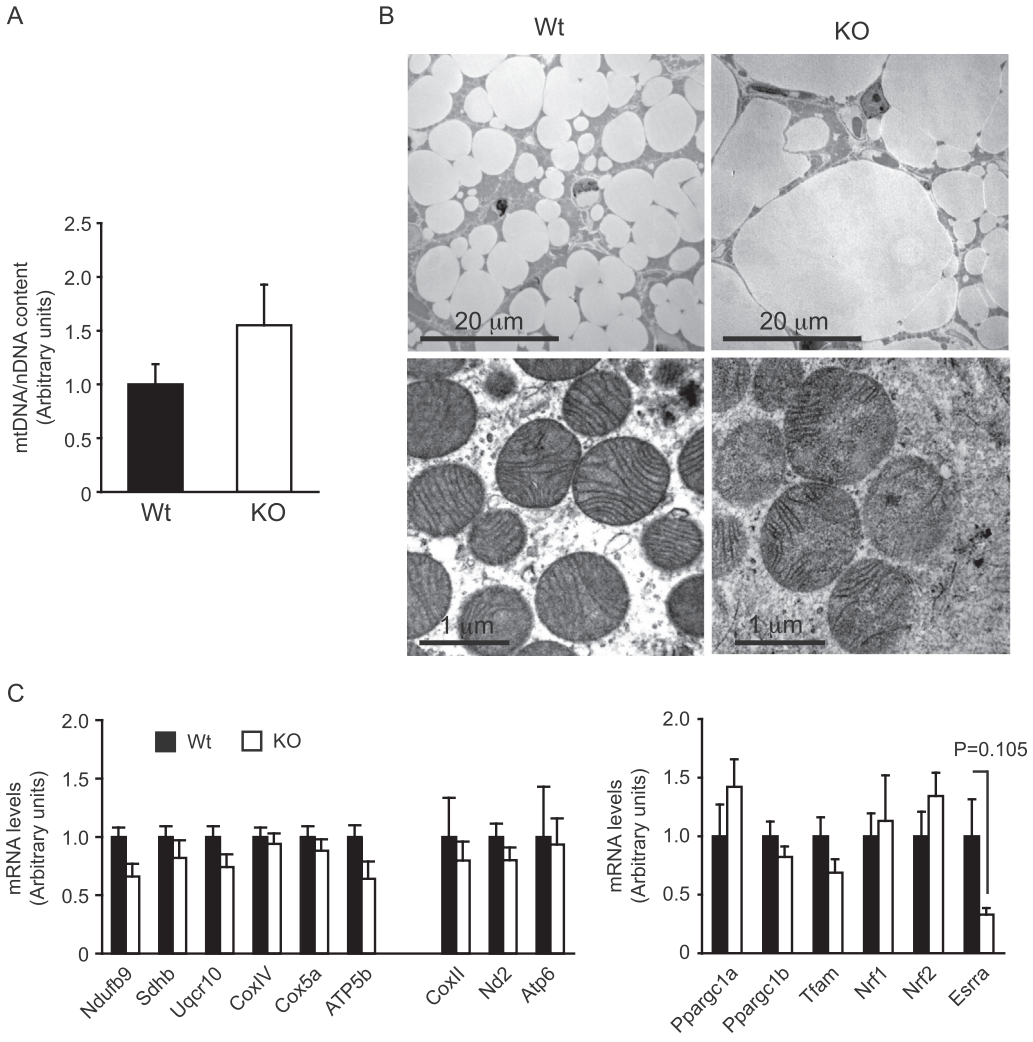

Fig. 4. MTERF4-FAT-KO mice do not exhibit a compensatory mitochondrial biogenic response in BAT. (A) Relative mtDNA content in BAT determined by real-time quantitative PCR was used as an indicator of mitochondrial mass. (B) Representative transmission electron microscopy images from 12-week old Wt and MTERF4-FAT-KO male mice fed a standard diet. (C) mRNA expression of nDNA- and mtDNA-encoded mitochondrial genes (left panel) and transcriptional regulators of mitochondrial biogenesis (right panel) was assessed by real-time quantitative PCR in BAT of 10- to 12-week old Wt and MTERF4-FAT-KO male mice fed a standard diet. Data are the mean ± SEM (n = 4–5 mice/group).

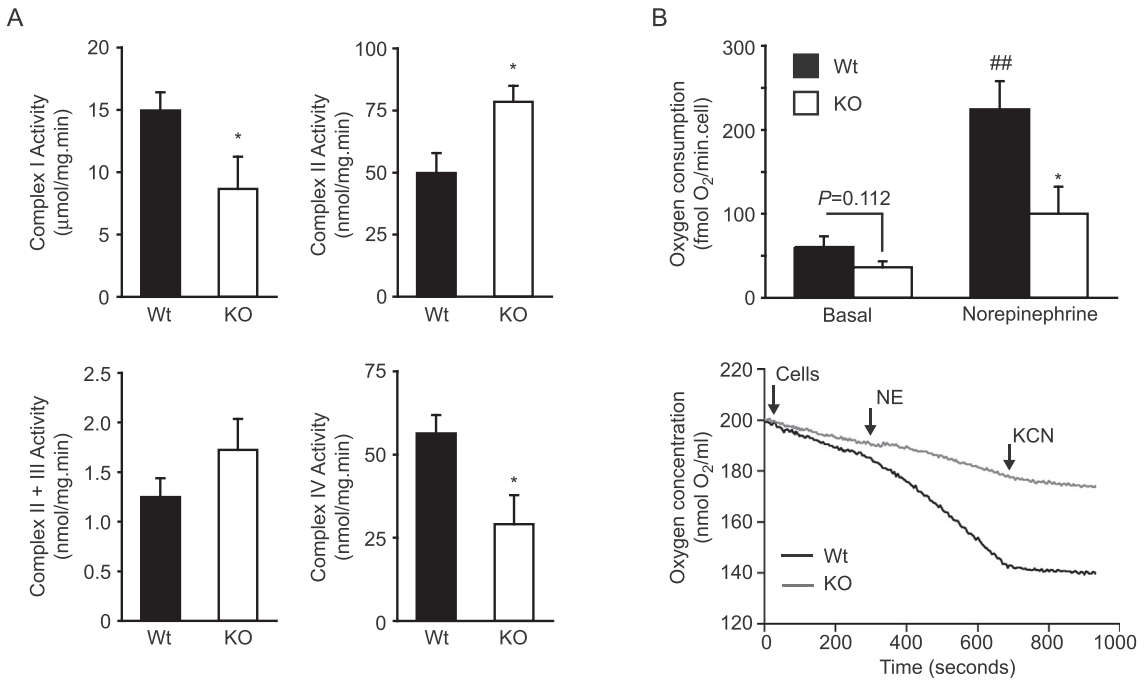

Fig. 5. Mitochondrial oxidative function of brown adipocytes is impaired in mice lacking MTERF4. (A) Enzymatic activity of mitochondrial respiratory chain complexes I-IV was measured by spectrophotometric methods in mitochondria isolated from BAT of 10- to 12-week old Wt and MTERF4-FAT-KO male mice (n = 7–9 animals/group). (B) Respiration of brown adipocytes isolated from 10-week old Wt and MTERF4-FAT-KO mice fed a standard diet was measured with a Clark-type oxygen electrode in the absence (basal) or presence of 1 µM norepinephrine (NE). Lower panel shows the raw data of a representative respiration experiment. Data are the mean ± SEM of four independent experiments. * indicates the statistical significance of the comparison between Wt and MTERF4-FAT-KO mice; # indicates the statistical significance of the comparison between basal and norepinephrine-induced oxygen consumption. *$P \leq 0.05$, **, $^{\#\#}P \leq 0.01$.

lacking MTERF4 exhibit a decrease in basal oxygen consumption compared to Wt, although differences did not reach statistical significance. Moreover, contrary to Wt brown adipocytes, which robustly respond to norepinephrine by increasing oxygen consumption by almost three fold, brown adipocytes from MTERF4-FAT-KO mice hardly responded to adrenergic stimulation and failed to increase oxygen consumption to the same levels as Wt adipocytes. Altogether, these results indicate that lack of MTERF4 impairs mitochondrial oxidative metabolism of brown adipocytes.

3.4. Impaired non-shivering adaptive thermogenesis and increased cold sensitivity in MTERF4-FAT-KO mice

Gross morphological examination of BAT revealed important differences between Wt and MTERF4-FAT-KO mice. Indeed, BAT from Wt mice exhibited the reddish color characteristic of a highly active BAT, whereas BAT from MTERF4-FAT-KO mice appeared paler, suggesting a high accumulation of triglycerides (Fig. 6A). These alterations were confirmed at the microscopic level (Figs. 4B and 6B). Indeed, brown adipocytes from Wt mice had the characteristic features of active thermogenic cells, with triglycerides accumulated in multiple and small vacuoles. Contrarily, BAT of MTERF4-FAT-KO mice exhibited the presence of numerous cells with a white adipocyte-like morphology, big in size and accumulating triglycerides in a single vacuole. The increased lipid accumulation together with the reduced mitochondrial oxidative capacity shown by brown adipocytes of MTERF4-FAT-KO mice strongly suggests a defect in BAT thermogenesis. As a first approach to determine BAT thermogenic activity in mice lacking MTERF4, we used infrared imaging to determine the surface temperature of the interscapular region, where the main BAT depot is located. As shown in Fig. 6C, the interscapular temperature of MTERF4-FAT-KO mice was almost 1 °C lower than in Wt mice.

Because BAT non-shivering thermogenesis is mediated through the sympathetic stimulation of β_3-adrenergic receptors, we tested by indirect calorimetry the thermogenic capacity of MTERF4-FAT-KO mice and Wt littermates by measuring oxygen consumption immediately after acute administration of the β_3-receptor specific agonist CL316,243. As shown in Fig. 6D, Wt responded to the β_3-receptor agonist by rapidly increasing oxygen consumption, whereas this response was severely blunted in MTERF4-FAT-KO mice.

BAT heavily relies on free-fatty acids released by WAT in response to adrenergic stimulation to carry thermogenesis [30]. This prompted us to determine if the impaired thermogenic capacity of MTERF4-FAT-KO mice was the result of an altered lipolytic response. Stimulation of lipolysis with isoproterenol similarly increased the circulating levels of FFA in Wt and MTERF4-FAT-KO mice, indicating that the capacity to mobilize lipidic substrates to sustain thermogenesis was not altered in mice lacking MTERF4 (Fig. 6E).

The physiological consequences of lacking MTERF4 in BAT were analyzed by acutely exposing mice to cold. When MTERF4-FAT-KO mice were exposed to 4 °C, they rapidly lost body temperature and became hypothermic (Fig. 7A). However, Wt littermates were able to maintain their body temperature throughout the duration of the experiment.

Consistent with the notion that impaired cold-induced thermogenesis in MTERF4-FAT-KO is the result of reduced mitochondrial oxidative capacity, brown adipocytes from mice lacking MTERF4 accumulate large amounts of triglycerides in their cytoplasm in single big vacuoles after being exposed to cold (Fig. 7B). Contrarily, brown adipocytes from Wt appeared almost completely depleted of lipids as a result of their oxidation to produce the heat required to maintain body temperature. Remarkably, we observed that the levels of UCP1 protein was very similar in BAT of Wt and MTERF4-FAT-KO mice prior to the exposure to low environmental temperatures (Fig. 7C), supporting the notion that impaired thermogenesis is the result of low OxPhos activity but not of alterations in UCP1 protein expression.

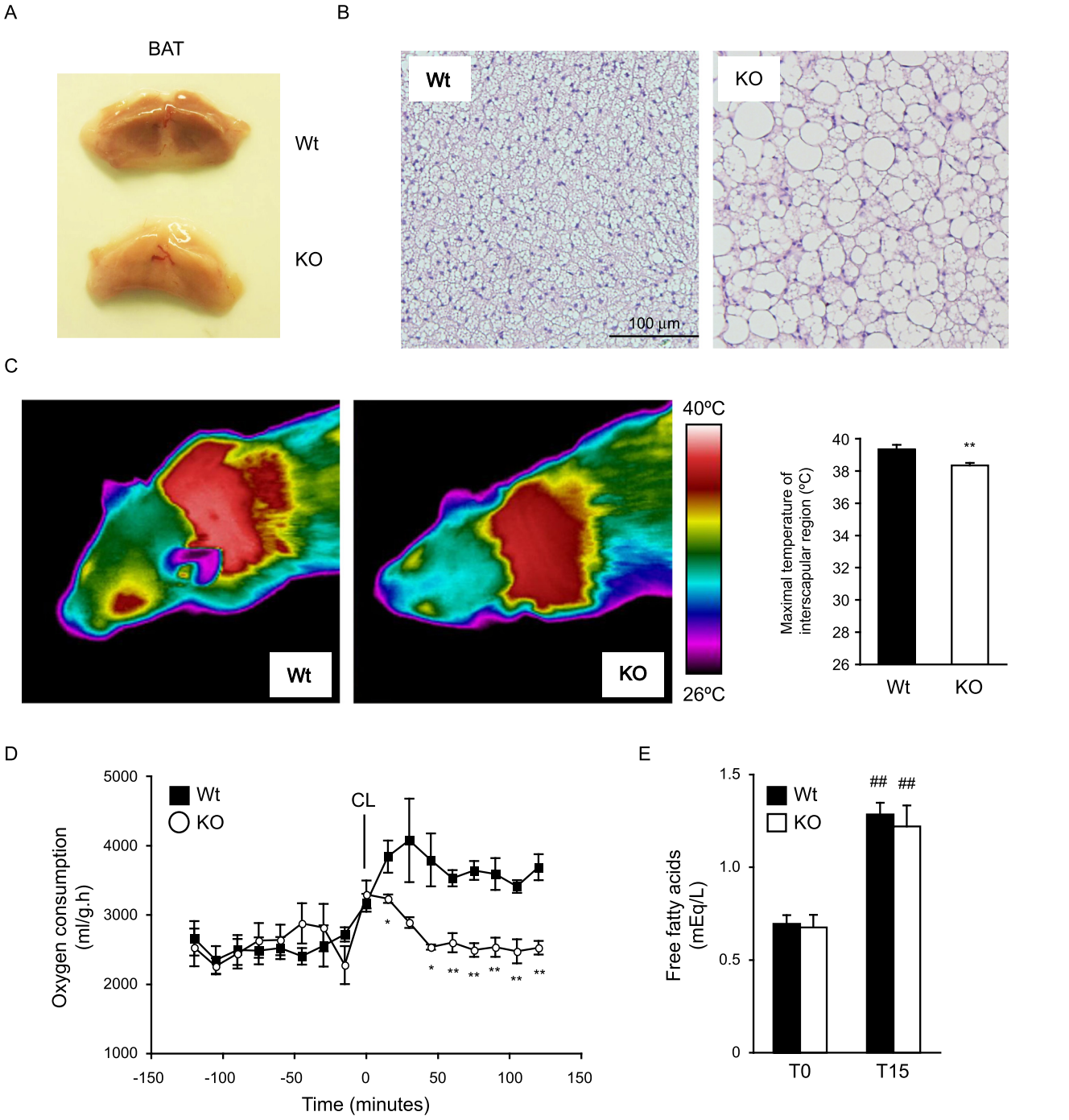

Fig. 6. Impaired BAT thermogenic function in MTERF4-FAT-KO mice. (A) Gross morphological aspect of BAT from 10-week old Wt and MTERF4-FAT-KO male mice fed a standard diet. (B) Histological sections of BAT stained with haematoxilin/eosin. (C) Surface temperature of the interscapular area was determined by infrared imaging (n = 6–7 mice/group). (D) CL-316,243-stimulated (1 mg/kg) oxygen consumption in Wt and MTERF4-FAT-KO mice fed a standard diet (n = 5–6 mice/group). (E) Lipolysis was evaluated by determining the levels of circulating FFA before (T0) and 15 min (T15) after an injection of isoproterenol (10 mg/Kg), (n = 7–8 mice/group). Data are the mean ± SEM. * indicates the statistical significance of the comparison between Wt and MTERF4-FAT-KO mice; # indicates the statistical significance of the comparison between basal and isoproterenol-induced lipolysis $^{*}P \leq 0.05$, **, $^{\#\#}P \leq 0.01$.

3.5. Lack of BAT function in MTERF4-FAT-KO mice does not affect energy balance or glucose homeostasis

Since impaired BAT function has been linked to obesity and insulin resistance, we aimed at studying how lack of MTERF4 and the consequent reduction in the oxidative capacity of brown adipocytes affected energy balance and glucose homeostasis. Indirect calorimetry in 11- to 12-week old mice revealed similar energy expenditure between Wt and MTERF4-FAT-KO mice, during both the light and dark phases of the diurnal period (Fig. 8A). Consistent with the absence of differences in energy expenditure, locomotor activity (Fig. 8B) or food intake (Fig. 8C), MTERF4-FAT-KO mice exhibited similar body weight (Fig. 8D and F) and fat content (Fig. 8E) than their Wt counterparts. Moreover, MTERF4-FAT-KO mice exhibited normal glucose tolerance and insulin sensitivity, despite the severe BAT dysfunction described (Fig. 8G–H). When animals were challenged with a high fat diet for 18 weeks, no differences were found between genotypes, since both Wt and MTERF4-FAT-KO mice similarly developed obesity, glucose intolerance and

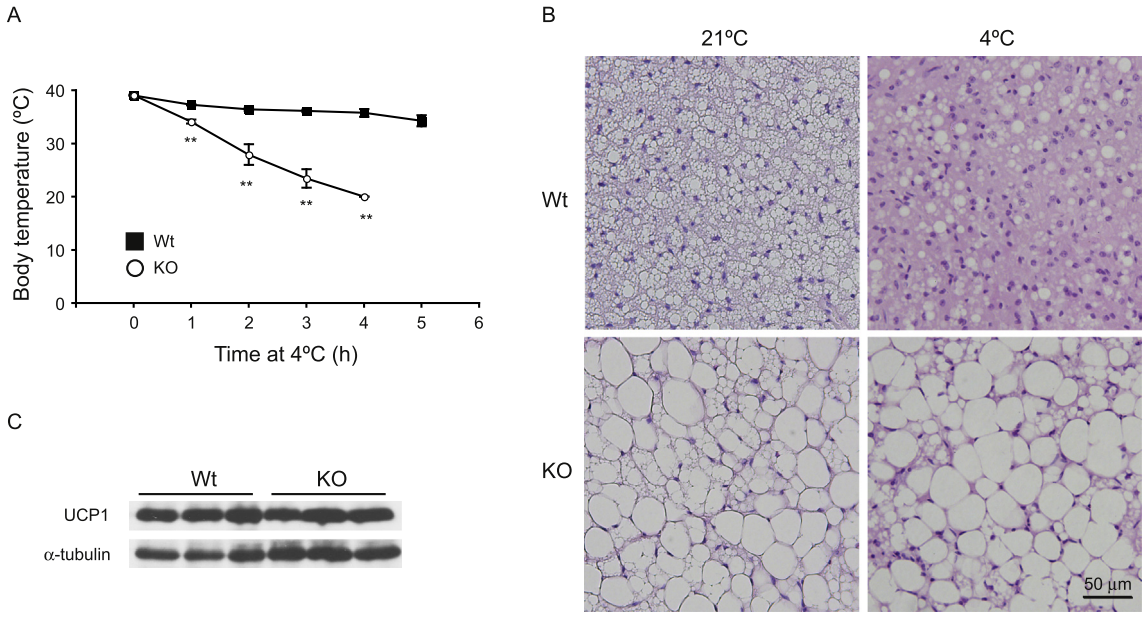

Fig. 7. MTERF4-FAT-KO mice are cold sensitive. (A) Body temperature of 9- to 10-week old Wt and MTERF4-FAT-KO male mice fed a standard diet exposed at 4 °C during 5 h. Data are the mean ± SEM (n = 5 mice/group; $^{**}P \leq 0.01$). (B) Histological analysis of BAT from Wt and MTERF4-FAT-KO mice housed at 21 °C or exposed at 4 °C for 5 h. (C) Western blot of UCP1 in BAT of Wt and MTERF4-FAT-KO mice (n = 3 mice/group) housed at 21 °C, before being exposed to cold.

insulin resistance (Fig. 9).

3.6. Resistance of MTERF4-FAT-KO mice to the amelioration of glucose homeostasis by chronic treatment with β_3-receptor agonist

Recruitment of new brown and beige adipocytes within BAT and WAT depots, respectively, and sustained activation of thermogenesis has been suggested as a potential therapeutic strategy for the treatment of obesity and associated metabolic diseases. To demonstrate to which extent thermogenic activation of brown adipocytes in BAT and beige adipocytes recruited in WAT are indeed required for the metabolic improvement in response to adrenergic stimulation, we first fed Wt and MTERF4-FAT-KO mice with a high fat diet to induce obesity and insulin resistance and then treated them for three weeks with the β_3-agonist CL316,243. Treatment with the β_3-adrenoreceptor specific agonist had no noticeable effect on the levels of mitochondrial proteins in BAT of Wt mice (Fig. 10A). Still, compared to Wt littermates, MTERF4-FAT-KO mice exhibited reduced levels, both under basal and adrenergic-stimulated conditions, of proteins belonging to OxPhos complexes I and IV, regardless of whether they were encoded by the mtDNA or nDNA. Contrarily, proteins of the OxPhos complex II (i.e. SDHB) were not affected by the lack of MTERF4 and were expressed in BAT at similar levels than in Wt animals. As expected, adrenergic stimulation of Wt mice strongly induced browning of WAT, as indicated by a remarkable induction of UCP1 expression (Fig. 10B). MTERF4-FAT-KO mice responded to the treatment with CL316,243 with a similar degree of WAT browning, as judged by similar levels of UCP1, as Wt mice (Fig. 10B). Browning of WAT was accompanied by an increase in the levels of mitochondrial proteins in both Wt and MTERF4-FAT-KO mice. However, consistent with previous observations in BAT, proteins encoded by the mtDNA or belonging to OxPhos complexes that contain mtDNA-encoded subunits (i.e. OxPhos complexes I and IV) were induced to a lower extent in WAT of MTERF4-FAT-KO mice. The noticeable induction of proteins like COXI after adrenergic stimulation in WAT of MTERF4-FAT-KO could be due to the responsiveness to CL stimulation of beige adipocytes in which recombination of the mterf4 gene has not occurred as a result of the variable recombination efficiency in our AdipoQ-Cre loxP model [31].

To study the effects of reduced brown and beige adipocyte oxidative capacity on glucose homeostasis in response to adrenergic stimulation, glucose and insulin tolerance tests were performed after the treatment with the β_3-adrenergic agonist. As shown in Fig. 10C–D, obese Wt mice responded to the treatment with CL316,243 by significantly improving glucose tolerance and insulin sensitivity. However, MTERF4-FAT-KO mice failed to respond to adrenergic stimulation and did not improve glucose homeostasis despite the efficient browning showed after the treatment with CL316,243. [^{18}F]-FDG uptake by BAT measured by PET revealed no differences between Wt and MTERF4-FAT-KO mice under basal conditions (Fig. 10E). Moreover, adrenergic stimulation with CL316,243 lead to a similar increase in glucose uptake in Wt and KO mice, suggesting that differential glucose clearance during the course of GTTs and ITTs in MTERF4-FAT-KO mice in response to β_3-adrenergic agonist treatment was independent of BAT glucose uptake. We also assessed the effect of β_3-agonist treatment on body weight. As shown in Fig. 10F, after 3 weeks of treatment with CL316,243 Wt mice decreased body weight by > 3 g. However, the decrease in body weight induced by the β_3 agonist was less pronounced in MTERF4-FAT-KO mice. Interestingly, CL316,243 preferentially induced a reduction in the weight of gonadal WAT, whereas it had minor effects on other WAT depots or liver (Fig. 10F). Still, no significant differences were found between Wt and MTERF4-FAT-KO mice.

4. Discussion

The discovery of active BAT in adult humans has brought renewed interest in this tissue as a potential therapeutic target for the treatment of obesity and its associated metabolic diseases by means of increasing energy expenditure. The capacity of brown adipocytes to dissipate energy as heat relies on the acquisition during the course of their differentiation of a dense network of mitochondria distinctively equipped with UCP1 [32,33]. The balanced acquisition of all the protein machinery of the respiratory chain is absolutely needed in order to build up the membrane electrochemical potential that will be dissipated by UCP1 to generate heat.

The present study demonstrates that MTERF4, a mitochondrial protein of the MTERF family of transcription termination factors, is essential for the full oxidative function of brown adipocytes. Our findings showing that lack of MTERF4 severely impairs the translation

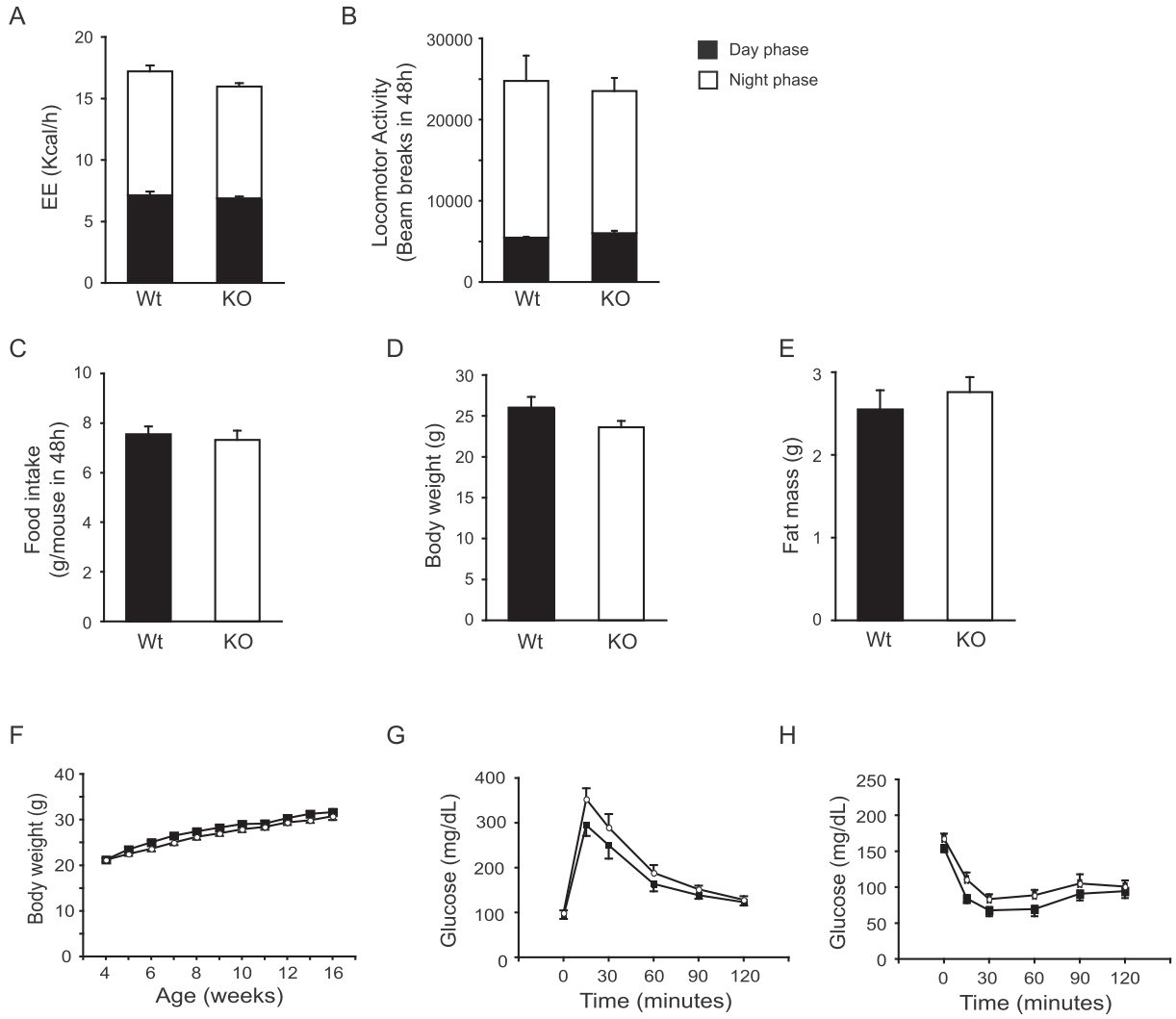

Fig. 8. Preserved energy balance and glucose homeostasis in mice lacking MTERF4 in adipose tissues. (A) Energy expenditure was determined by indirect calorimetry. (B) Locomotor activity. (C) Food intake. (D) Body weight of mice before the calorimetric measurements. (E) Fat mass was determined by NMR. (F) Follow up of body weight during 12 weeks. (G) Glucose tolerance test was performed after a 12 h fast and with a dose of 2 g/Kg of glucose. (H) Insulin tolerance test was performed in 5 h fasted mice and a dose of 0.75 U/Kg of insulin. All experiments were conducted in 8- to 10-week old male mice fed a standard chow diet, except for the glucose and insulin tolerance tests that were performed on 16-week old male mice. Data are the mean ± SEM (n = 5–6 mice/group).

of proteins encoded by the mitochondrial genome in brown adipocytes fully supports the current view of MTERF4 as a central factor for mitochondrial protein translation. Indeed, the current action model for MTERF4 proposes that it controls mitochondrial protein translation by participating in mitochondrial ribogenesis [22]. Specifically, MTERF4 would form a complex with NSUN4, another mitochondrial protein with methyltransferase activity, and facilitate its recruitment to the large mitochondrial ribosome subunit. The MTERF4/NSUN4 complex would enable the interaction and subsequent assembly of the large and small mitochondrial ribosomal subunits to form fully functional mitoribosomes [23]. Although our results strongly support a critical role of MTERF4 mitoribogenesis and protein translation, some variable but still detectable translation of mtDNA-encoded genes was detected in BAT of mice devoid of MTERF4. The detection of some basal translation of mtDNA-encoded proteins could be explained by the translational activity in adipocytes in which efficient recombination of the *Mterf4* gene has not occurred [31]. Residual translation is also compatible with some degree of mitoribogenesis still occurring in the absence of MTERF4 [22], suggesting that other factors may contribute to the assembly of mitochondrial ribosomes to ensure certain basal level of mitochondrial protein translation.

Although MTERF4 exclusively controls the translation of mtDNA-encoded proteins, the levels of protein subunits encoded by the nDNA but belonging to OxPhos complexes composed by both nDNA- and mtDNA-encoded proteins were found reduced in BAT of MTERF4-FAT-KO mice. mtDNA-encoded OxPhos subunits are highly hydrophobic proteins residing in the inner mitochondrial membrane and act as seeding cores for the assembly of the rest of the subunits that form the functional OxPhos complex. In this regard, given the defect in their translation in the absence of MTERF4, mtDNA-encoded proteins become limiting for the stoichiometric assembly of the OxPhos complexes. As a result, the unassembled subunits are eventually degraded to avoid their accumulation within the adipocytes of MTERF4-FAT-KO mice [34]. As a consequence, the loss of MTERF4 in BAT leads to a net decrease of approximately 40–60% in the levels of assembled OxPhos complexes I, III and IV that translates into a similar reduction in their enzymatic activity and an overall decreased in the oxidative capacity of brown adipocytes, both under basal conditions and upon adrenergic stimulation.

The primary physiological defect that stems from ablation of MTERF4 in adipose tissues is the severe cold intolerance exhibited by MTERF4-FAT-KO mice when acutely exposed to low temperatures. The

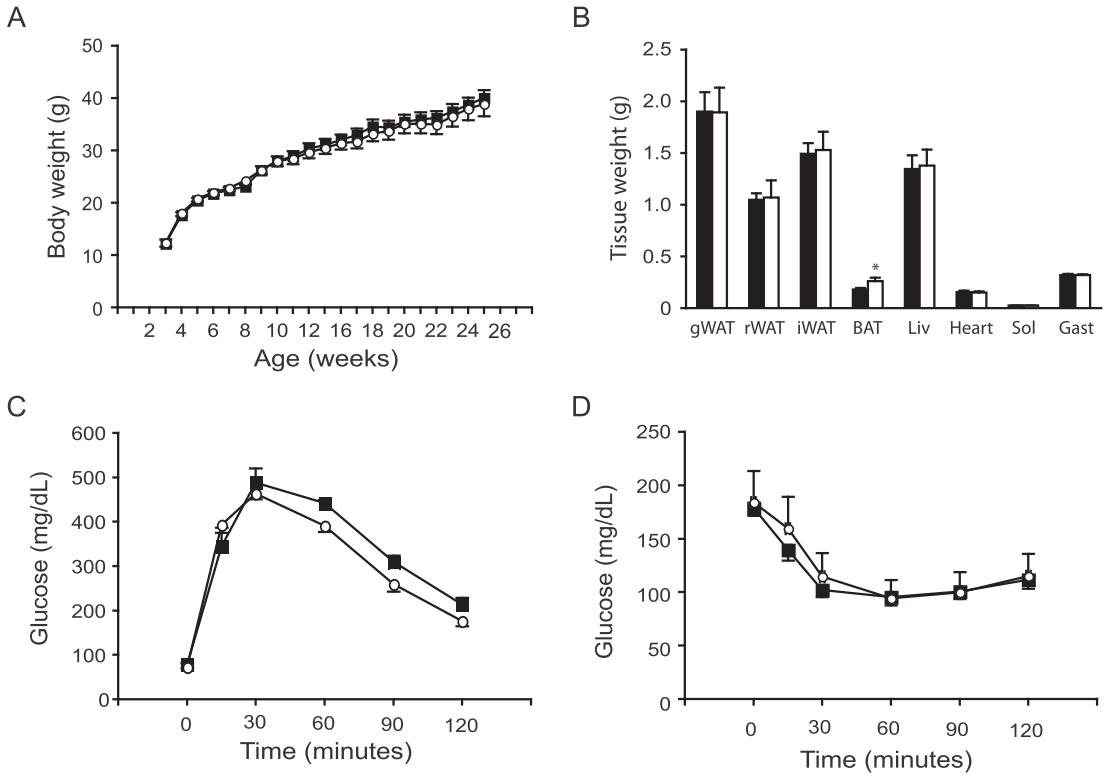

Fig. 9. Effects of a high fat diet on body weight and glucose homeostasis in mice lacking MTERF4 in adipose tissues. Wt and MTERF4-FAT-KO mice were fed a high fat diet (60% Kcal from fat) for 18 weeks, starting at the age of 8 weeks. (A) Body weight was determined weekly during the duration of the experiment. (B) At 26 weeks of age, mice were euthanized and tissues weighted (gWAT, gonadal WAT; rWAT, retroperitoneal WAT; iWAT, inguinal WAT; Liv, Liver; Sol, soleus; Gast, gastrocnemious). (C) Glucose tolerance test was performed on 12 h-fasted mice (2 g/Kg glucose) (D) Insulin tolerance test was performed on 5 h-fasted mice (0.85 U/Kg insulin). Data are the mean ± SEM (n = 6–8 mice/group).

reduced capacity for cold-induced thermogenesis is neither due to inadequate UCP1 expression -MTERF4-FAT-KO mice exhibit similar levels of UCP1 than their Wt littermates- nor to a reduced capacity to mobilize fatty acids by lipolysis. Although lipolysis is critical for BAT thermogenesis, it has been shown that mice with defective lipolysis specifically in brown adipocytes have their cold-induced thermogenic capacity preserved due to the capacity to use fatty acids released by white adipocytes as thermogenic substrates [30,35]. Therefore, even if the increased triglyceride accumulation observed in BAT of MTERF4-FAT-KO mice would suggest an impaired brown adipocyte lipolytic capacity, the similar response of Wt and MTERF4-FAT-KO mice to isoproterenol in raising the circulating levels of free fatty acids indicates that the availability of lipid substrates for thermogenesis is guaranteed despite the lack of MTERF4. Consequently, our results unequivocally point towards the reduced respiratory chain complex activity as the major cause of the cold intolerance exhibited by MTERF4-FAT-KO mice, which are unable to build up the mitochondrial electrochemical gradient required by UCP1 to carry out thermogenesis.

The mitochondrial defects in BAT of MTERF4-FAT-KO mice are reminiscent of those found in heart of cardiac-specific MTERF4 knockout mice, which show reduced assembly and activity of OxPhos complexes I, III, IV and V, as well as low content of mtDNA-encoded proteins and reduced levels of some nDNA-encoded subunits [22]. The pathophysiological result of the loss of MTERF4 in heart is the development of a severe cardiomyopathy that leads to premature death around 21 weeks of age, as a direct consequence of the disruption of proper mitochondrial function. A major difference between the cardiac- and our adipose-specific knockout models lies in the transcriptional response to impaired mitochondrial function. Indeed, in heart of cardiac-specific knockout mice, a noticeable increase in the levels mtDNA-encoded RNAs was found [22], suggesting the activation of a mitochondrial biogenic response aimed at compensating mitochondrial dysfunction and maintaining cardiac function. In this line, a dramatic increase mitochondrial mass was observed in cardiac muscle of heart-specific MTERF4-KO mice, which show aberrant mitochondria arranged in a disorganized manner within the cardiac muscle fibers. However, the lack of such compensatory mitochondriogenic response in BAT, despite the severe defect in its oxidative function, together with the fact that MTERF4-FAT-KO mice maintain normal energy expenditure and body temperature when housed at 21 °C suggest that mice can adapt to defective BAT thermogenesis by recruiting other thermogenic mechanisms that overtake the function of inactive BAT. Therefore, whereas a mitochondriogenic response in heart of cardiac-specific MTERF4-KO mice is absolutely required as an attempt to maintain heart function at any cost, such response might be dispensable in BAT, since brown adipocyte thermogenesis could be substituted by alternative thermogenic mechanisms [36]. Thus, under normal housing conditions (21 °C), the mitochondria with smaller cristae and reduced OxPhos complexes content of MTERF4-FAT-KO mice appear sufficient to sustain viable brown adipocytes. However, when animals are exposed to cold, the newly recruited thermogenic mechanisms are insufficient to maintain the production of heat required to maintain body temperature and MTERF4-FAT-KO mice get into hypothermia. The MTERF4-FAT-KO phenotype would be similar to that observed in UCP1 knockout mice, which, despite of exhibiting impaired BAT non-shivering adaptive thermogenesis due to the lack of UCP1, they adapt to low temperatures by increasing shivering [33]. The recruitment of other recently described processes with thermogenic potential, such as creatine futile cycle [37] or the generation of endogenous n-acyl amino acids with uncoupling properties [38] in MTERF4-FAT-KO mice cannot be disregarded and would deserve further investigation. Moreover, it would be interesting to investigate if long term adaptation to mildly cold

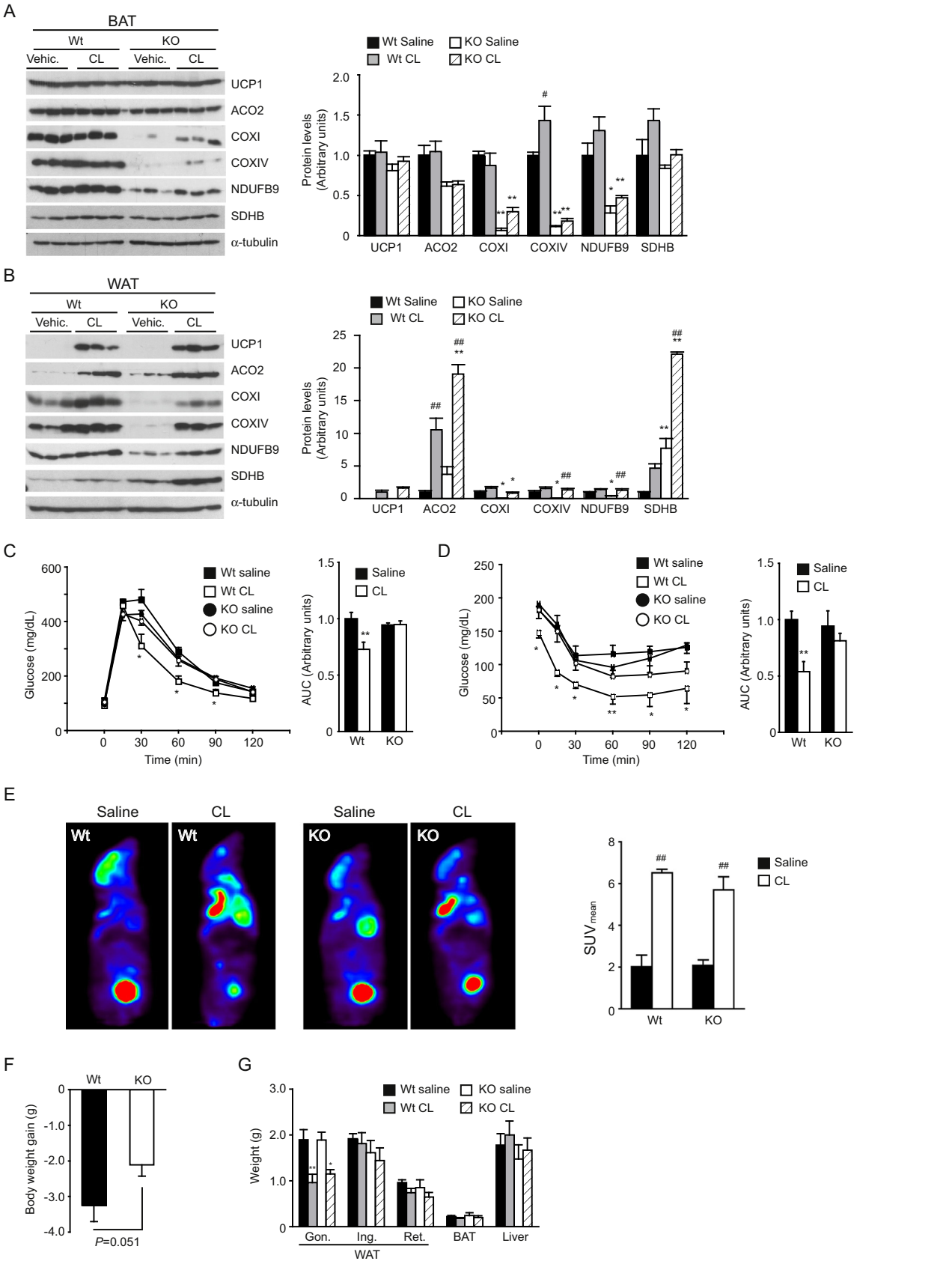

(caption on next page)

Fig. 10. Effect of long-term β_3-adrenergic stimulation on glucose homeostasis in Wt and MTERF4-FAT-KO mice fed a high fat diet. Wt and MTERF4-FAT-KO mice were fed a high fat diet (60% kcal from fat) during 15 weeks, starting at the age of 8 weeks. After 12 weeks on a high fat diet, mice were treated during 3 weeks with a daily dose 1 mg/Kg of CL316,243 or saline. (A) Western blots of mitochondrial proteins in BAT. Densitometric quantification of immunoblots is shown in the right panel. (B) Western blots of mitochondrial proteins in WAT. Densitometric quantification of immunoblots is shown in the right panel. (C) Glucose tolerance test was performed on 12 h-fasted mice (2 g/Kg glucose). The area under the curve is shown on the right panel. (D) Insulin tolerance test was performed on 5 h-fasted mice (0.85 U/Kg insulin). The area under the curve is shown on the right panel. (E) PET scanning of [^{18}F]-FDG uptake by BAT in 15-week old male mice fed a standard diet. (F) Body weight gain in Wt and MTERF4-FAT-KO mice after the 3-week treatment with CL316,243. (E) Weight of major WAT depots, BAT and liver in mice subjected to long term treatment with CL316,243. Data are the mean ± SEM (n = 4–5 mice/group). * indicates the statistical significance of the comparison between Wt and MTERF4-FAT-KO mice; # indicates the statistical significance of the comparison between saline and CL-treatment; $^{*,\#}P \leq 0.05$, $^{**,\#\#}P \leq 0.01$.

temperatures is sufficient to mount the mitochondriogenic response that was not observed under the temperature conditions used in the present study.

Owing to its high oxidative capacity, BAT may exert a notable influence on energy balance [39,40]. Lower BAT mass and activity in adult humans is associated with increased body mass index and blood glucose levels [8,9], suggesting that impaired BAT oxidative function may predispose to the development of obesity and glucose metabolism disturbances. Surprisingly, MTERF4-FAT-KO mice do not gain more weight than their Wt littermates nor they exhibit any alteration in glucose homeostasis, even when fed an obesogenic diet. The lack of differences in body weight between Wt and MTERF4-FAT-KO mice clearly indicate that whole body energy balance is preserved in mice lacking MTERF4, despite the severe impairment in BAT oxidative function observed. This is consistent with the absence of differences in energy expenditure and food intake between Wt and MTERF4-FAT-KO mice. These, somehow, surprising findings are in line with the results of other studies in rodent models devoid of genes like *Ucp1* [32], *Hdac3* [41] or *Cpt2* [42] specifically in adipocytes. All these mouse models are characterized by deficient thermogenesis and exacerbated cold sensitivity, but none of them become obese, even if fed a high fat diet. Altogether, these studies seem to undermine the contribution of BAT to whole body energy expenditure. However, they are compatible with recent studies that describe the recruitment of alternative thermogenic mechanisms aimed at maintaining body temperature under standard housing conditions in mice devoid of UCP1-dependent BAT non-shivering thermogenesis. As mentioned above, different futile cycles or alternative thermogenic mechanisms that contribute to energy expenditure and heat production have been described in other tissues [37,38,43,44]. Nevertheless, the contribution of these UCP1-independent thermogenic mechanisms to whole body energy balance has not been explored in humans.

On the other hand, it has been proposed that that BAT-dependent diet-induced thermogenesis greatly contributes to the maintenance of body weight. Thus, at thermoneutrality, in the absence of any thermal stress that requires of thermogenic processes to maintain body temperature, UCP1 knockout mice develop obesity [45,46]. However, BAT-dependent diet-induced remains a controversial issue [47,48] and some other mouse models exhibiting severe BAT thermogenesis deficiency due to lack of key genes involved in energy metabolism, such as *Esrra/Esrrg* [13] or *Cpt2* [49], do not develop obesity at thermoneutrality. Therefore, although it is conceivable to speculate that MTERF4-FAT-KO mice would develop obesity under thermoneutral conditions as a result of impaired thermogenesis induced by diet, such hypothesis would need to be corroborated in future studies.

Regardless of whether lack of basal thermogenic activity in brown adipocytes is sufficient to bring about a deleterious metabolic phenotype, many studies in rodents support the notion that enhanced activation of BAT and browning of WAT greatly influence energy balance and prevent obesity and obesity-related metabolic diseases, like insulin resistance or type 2 diabetes [7,50]. In humans, evidence that boosted activity of BAT has positive metabolic effects come from patients with hibernomas or pheochromocytomes, who show abnormally increased BAT mass and activity in correlation with reduced body weight [51,52]. Also, BAT activation by cold exposure in adult humans has been shown to significantly increase energy expenditure and to improve whole body insulin sensitivity [53,54]. Therefore, brown and beige adipocytes have been viewed as an appealing target for the treatment of metabolic diseases. Our findings that Wt mice but not MTERF4-FAT-KO fed a high fat diet respond to treatment with the β_3-receptor agonist CL316,243 by increasing oxygen consumption and improving glucose homeostasis are in full support of this idea. Again, the blunted response to the treatment with CL316,243 observed in MTERF4-FAT-KO is not the result of impaired UCP1 expression in BAT, since both Wt and MTERF4-FAT-KO mice exhibit similar levels of the protein in response to adrenergic stimulation. Similarly, the browning capacity of WAT, as judged by the induction of UCP1 protein, is preserved in MTERF4-FAT-KO mice. Remarkably, the similar glucose uptake capacity exhibited by BAT of Wt and MTERF4-FAT-KO mice when treated with a β_3-receptor agonist strongly suggests that the blunted improvement in glucose homeostasis exhibited by mice lacking MTERF4 is not due differential glucose uptake capacity in BAT. While glucose uptake has been often used as readout of BAT thermogenesis, our results are in line with recent reports that demonstrate a dissociation between adrenergically-induced glucose uptake and thermogenesis [55]. The lack of improvement in glucose homeostasis and reduction in body weight clearly seems to be the result of the incapacity of adrenergic stimulation by β_3-adrenergic receptor specific agonists to increase energy expenditure in brown and beige adipocytes. Although we did not measure it, the glucose uptake attributable to beige adipocytes is not expected to be different between Wt and MTERF4-FAT-KO mice, since both beige and brown adipocytes, despite their different ontogenic origin, similarly respond to adrenergic stimulation by activating UCP1-depedent thermogenesis [6]. Still, given the reduced mitochondrial OxPhos protein content in WAT as a result of the lack of MTERF4, a potential contribution of white adipocytes to the differential metabolic response to adrenergic stimulation cannot be totally ruled out. Our findings are similar to those reported in a recent study using mice simultaneously devoid of ERRα and ERRγ, two orphan hormone nuclear receptors that redundantly regulate mitochondrial biogenesis in brown/beige adipocytes. ERRα/γ adipose-specific double knockout exhibit impaired thermogenesis and are refractory to the metabolic effects of adrenergic stimulation. As a result, they do not improve glucose homeostasis nor they reduced body weight in response to CL316,243 to the same extent as their Wt counterparts [13]. Altogether, these findings strongly suggest that pharmacological activation of brown/beige adipocytes by the use of sympathomimetics would be sufficient to revert diet-induced insulin resistance in humans. However, the undesirable cardiovascular side effects (i.e. rise in blood pressure and heart rate) associated with the therapeutic doses of adrenergic receptor agonists used in the clinical practice preclude their use in obese and diabetic patients [56,57]. In this regard, several new molecules, including fibroblast growth factor 21, natriuretic peptides, bone morphogenic proteins or capsinoids, with the capacity to recruit and activate brown adipocytes have been identified, but their therapeutic potential remain to be defined (reviewed in [7,58]).

In summary, our results demonstrate that MTERF4 regulates mtDNA-encoded protein translation in BAT. We also show that MTERF4 is essential for the thermogenic function of brown adipocytes in response to cold, although impaired BAT activity does not favor the spontaneous development of metabolic diseases in response to high fat diet. In addition, we provide strong evidence that pharmacological activation of brown/beige adipocytes may be an efficacious therapeutic

option for the treatment of insulin resistance and type 2 diabetes.

Supplementary data to this article can be found online at https://doi.org/10.1016/j.bbadis.2019.01.025.

Transparency document

The Transparency document associated with this article can be found in online version.

Acknowledgments

We thank Dr. N.G. Larsson for providing the *Mterf4* floxed mice and Dr. F. Villarroya for the use of the T420 Compact-Infrared-Thermal-Imaging-Camera. We also thank the Unit-20 of CIBER-BBN from the ICTS "Nanobiosis" for preparing the paraffin blocks used for histological analysis and the Microscopy Service from the "Universitat Autonoma de Barcelona" for their help with transmission electron microscopy.

Funding sources

This work was supported by grants SAF2012-39484 and BFU2015-64462R from the Ministerio de Economía y Competitividad (MINECO/FEDER, UE) to J.A.V.

Declaration of interest

None.

References

[1] B. Cannon, J. Nedergaard, Brown adipose tissue: function and physiological significance, Physiol. Rev. 84 (1) (2004) 277–359.
[2] D.G. Nicholls, R.M. Locke, Thermogenic mechanisms in brown fat, Physiol. Rev. 64 (1) (1984) 1–64.
[3] B. Cousin, S. Cinti, M. Morroni, S. Raimbault, D. Ricquier, L. Penicaud, et al., Occurrence of brown adipocytes in rat white adipose tissue: molecular and morphological characterization, J. Cell Sci. 103 (Pt 4) (1992) 931–942.
[4] A. Frontini, S. Cinti, Distribution and development of brown adipocytes in the murine and human adipose organ, Cell Metab. 11 (4) (2010) 253–256.
[5] P. Seale, S. Kajimura, W. Yang, S. Chin, L.M. Rohas, M. Uldry, et al., Transcriptional control of brown fat determination by PRDM16, Cell Metab. 6 (1) (2007) 38–54.
[6] I.G. Shabalina, N. Petrovic, J.M. de Jong, A.V. Kalinovich, B. Cannon, J. Nedergaard, UCP1 in brite/beige adipose tissue mitochondria is functionally thermogenic, Cell Rep. 5 (5) (2013) 1196–1203.
[7] M. Harms, P. Seale, Brown and beige fat: development, function and therapeutic potential, Nat. Med. 19 (10) (2013) 1252–1263.
[8] A.M. Cypess, S. Lehman, G. Williams, I. Tal, D. Rodman, A.B. Goldfine, et al., Identification and importance of brown adipose tissue in adult humans, N. Engl. J. Med. 360 (15) (2009) 1509–1517.
[9] M. Matsushita, T. Yoneshiro, S. Aita, T. Kameya, H. Sugie, M. Saito, Impact of brown adipose tissue on body fatness and glucose metabolism in healthy humans, Int. J. Obes. 38 (6) (2014) 812–817.
[10] M. Uldry, W. Yang, J. St-Pierre, J. Lin, P. Seale, B.M. Spiegelman, Complementary action of the PGC-1 coactivators in mitochondrial biogenesis and brown fat differentiation, Cell Metab. 3 (5) (2006) 333–341.
[11] J.A. Villena, M.C. Carmona, M. Rodriguez de la Concepcion, M. Rossmeisl, O. Vinas, T. Mampel, et al., Mitochondrial biogenesis in brown adipose tissue is associated with differential expression of transcription regulatory factors, Cell. Mol. Life Sci. 59 (11) (2002) 1934–1944.
[12] J.A. Villena, O. Vinas, T. Mampel, R. Iglesias, M. Giralt, F. Villarroya, Regulation of mitochondrial biogenesis in brown adipose tissue: nuclear respiratory factor-2/GA-binding protein is responsible for the transcriptional regulation of the gene for the mitochondrial ATP synthase beta subunit, Biochem. J. 331 (Pt 1) (1998) 121–127.
[13] E.L. Brown, B.C. Hazen, E. Eury, J.S. Wattez, M.L. Gantner, V. Albert, et al., Estrogen-related receptors mediate the adaptive response of Brown adipose tissue to adrenergic stimulation, iScience 2 (2018) 221–237.
[14] J.A. Villena, M.B. Hock, W.Y. Chang, J.E. Barcas, V. Giguere, A. Kralli, Orphan nuclear receptor estrogen-related receptor alpha is essential for adaptive thermogenesis, Proc. Natl. Acad. Sci. U. S. A. 104 (4) (2007) 1418–1423.
[15] C.J. Lelliott, G. Medina-Gomez, N. Petrovic, A. Kis, H.M. Feldmann, M. Bjursell, et al., Ablation of PGC-1beta results in defective mitochondrial activity, thermogenesis, hepatic function, and cardiac performance, PLoS Biol. 4 (11) (2006) e369.
[16] J. Lin, P.H. Wu, P.T. Tarr, K.S. Lindenberg, J. St-Pierre, C.Y. Zhang, et al., Defects in adaptive energy metabolism with CNS-linked hyperactivity in PGC-1alpha null mice, Cell 119 (1) (2004) 121–135.
[17] C.M. Gustafsson, M. Falkenberg, N.G. Larsson, Maintenance and expression of mammalian mitochondrial DNA, Annu. Rev. Biochem. 85 (2016) 133–160.
[18] M. Terzioglu, B. Ruzzenente, J. Harmel, A. Mourier, E. Jemt, M.D. Lopez, et al., MTERF1 binds mtDNA to prevent transcriptional interference at the light-strand promoter but is dispensable for rRNA gene transcription regulation, Cell Metab. 17 (4) (2013) 618–626.
[19] T. Wenz, C. Luca, A. Torraco, C.T. Moraes, mTERF2 regulates oxidative phosphorylation by modulating mtDNA transcription, Cell Metab. 9 (6) (2009) 499–511.
[20] C.B. Park, J. Asin-Cayuela, Y. Camara, Y. Shi, M. Pellegrini, M. Gaspari, et al., MTERF3 is a negative regulator of mammalian mtDNA transcription, Cell 130 (2) (2007) 273–285.
[21] A. Wredenberg, M. Lagouge, A. Bratic, M.D. Metodiev, H. Spahr, A. Mourier, et al., MTERF3 regulates mitochondrial ribosome biogenesis in invertebrates and mammals, PLoS Genet. 9 (1) (2013) e1003178.
[22] Y. Camara, J. Asin-Cayuela, C.B. Park, M.D. Metodiev, Y. Shi, B. Ruzzenente, et al., MTERF4 regulates translation by targeting the methyltransferase NSUN4 to the mammalian mitochondrial ribosome, Cell Metab. 13 (5) (2011) 527–539.
[23] M.D. Metodiev, H. Spahr, P. Loguercio Polosa, C. Meharg, C. Becker, J. Altmueller, et al., NSUN4 is a dual function mitochondrial protein required for both methylation of 12S rRNA and coordination of mitoribosomal assembly, PLoS Genet. 10 (2) (2014) e1004110.
[24] J. Eguchi, X. Wang, S. Yu, E.E. Kershaw, P.C. Chiu, J. Dushay, et al., Transcriptional control of adipose lipid handling by IRF4, Cell Metab. 13 (3) (2011) 249–259.
[25] R. Pardo, N. Blasco, M. Vila, D. Beiroa, R. Nogueiras, X. Canas, et al., EndoG knockout mice show increased brown adipocyte recruitment in white adipose tissue and improved glucose homeostasis, Endocrinology 157 (10) (2016) 3873–3887.
[26] R. Pardo, N. Enguix, J. Lasheras, J.E. Feliu, A. Kralli, J.A. Villena, Rosiglitazone-induced mitochondrial biogenesis in white adipose tissue is independent of peroxisome proliferator-activated receptor gamma coactivator-1alpha, PLoS One 6 (11) (2011) e26989.
[27] A.M. Loening, S.S. Gambhir, AMIDE: a free software tool for multimodality medical image analysis, Mol. Imaging 2 (3) (2003) 131–137.
[28] H. Schagger, G. von Jagow, Blue native electrophoresis for isolation of membrane protein complexes in enzymatically active form, Anal. Biochem. 199 (2) (1991) 223–231.
[29] N. Enguix, R. Pardo, A. Gonzalez, V.M. Lopez, R. Simo, A. Kralli, et al., Mice lacking PGC-1beta in adipose tissues reveal a dissociation between mitochondrial dysfunction and insulin resistance, Mol. Metab. 2 (3) (2013) 215–226.
[30] H. Shin, Y. Ma, T. Chanturiya, Q. Cao, Y. Wang, A.K.G. Kadegowda, et al., Lipolysis in Brown adipocytes is not essential for cold-induced thermogenesis in mice, Cell Metab. 26 (5) (2017) 764–777 (e765).
[31] K.Y. Lee, S.J. Russell, S. Ussar, J. Boucher, C. Vernochet, M.A. Mori, et al., Lessons on conditional gene targeting in mouse adipose tissue, Diabetes 62 (3) (2013) 864–874.
[32] S. Enerback, A. Jacobsson, E.M. Simpson, C. Guerra, H. Yamashita, M.E. Harper, et al., Mice lacking mitochondrial uncoupling protein are cold-sensitive but not obese, Nature 387 (6628) (1997) 90–94.
[33] V. Golozoubova, E. Hohtola, A. Matthias, A. Jacobsson, B. Cannon, J. Nedergaard, Only UCP1 can mediate adaptive nonshivering thermogenesis in the cold, FASEB J. 15 (11) (2001) 2048–2050.
[34] A. Timon-Gomez, E. Nyvltova, L.A. Abriata, A.J. Vila, J. Hosler, A. Barrientos, Mitochondrial cytochrome c oxidase biogenesis: recent developments, Semin. Cell Dev. Biol. 76 (2018) 163–178.
[35] G. Haemmerle, A. Lass, R. Zimmermann, G. Gorkiewicz, C. Meyer, J. Rozman, et al., Defective lipolysis and altered energy metabolism in mice lacking adipose triglyceride lipase, Science 312 (5774) (2006) 734–737.
[36] E.T. Chouchani, L. Kazak, B.M. Spiegelman, New advances in adaptive thermogenesis: UCP1 and beyond, Cell Metab. 29 (1) (2019) 27–37.
[37] L. Kazak, E.T. Chouchani, M.P. Jedrychowski, B.K. Erickson, K. Shinoda, P. Cohen, et al., A creatine-driven substrate cycle enhances energy expenditure and thermogenesis in beige fat, Cell 163 (3) (2015) 643–655.
[38] J.Z. Long, K.J. Svensson, L.A. Bateman, H. Lin, T. Kamenecka, I.A. Lokurkar, et al., The secreted enzyme PM20D1 regulates lipidated amino acid uncouplers of mitochondria, Cell 166 (2) (2016) 424–435.
[39] N.J. Rothwell, M.J. Stock, Luxuskonsumption, diet-induced thermogenesis and brown fat: the case in favour, Clin. Sci. (Lond.) 64 (1) (1983) 19–23.
[40] K.A. Virtanen, M.E. Lidell, J. Orava, M. Heglind, R. Westergren, T. Niemi, et al., Functional brown adipose tissue in healthy adults, N. Engl. J. Med. 360 (15) (2009) 1518–1525.
[41] M.J. Emmett, H.W. Lim, J. Jager, H.J. Richter, M. Adlanmerini, L.C. Peed, et al., Histone deacetylase 3 prepares brown adipose tissue for acute thermogenic challenge, Nature 546 (7659) (2017) 544–548.
[42] J. Lee, J.M. Ellis, M.J. Wolfgang, Adipose fatty acid oxidation is required for thermogenesis and potentiates oxidative stress-induced inflammation, Cell Rep. 10 (2) (2015) 266–279.
[43] R. Anunciado-Koza, J. Ukropec, R.A. Koza, L.P. Kozak, Inactivation of UCP1 and the glycerol phosphate cycle synergistically increases energy expenditure to resist diet-induced obesity, J. Biol. Chem. 283 (41) (2008) 27688–27697.
[44] L. Kazak, E.T. Chouchani, G.Z. Lu, M.P. Jedrychowski, C.J. Bare, A.I. Mina, et al., Genetic depletion of adipocyte creatine metabolism inhibits diet-induced thermogenesis and drives obesity, Cell Metab. 26 (4) (2017) 660–671 (e663).
[45] H.M. Feldmann, V. Golozoubova, B. Cannon, J. Nedergaard, UCP1 ablation induces obesity and abolishes diet-induced thermogenesis in mice exempt from thermal stress by living at thermoneutrality, Cell Metab. 9 (2) (2009) 203–209.
[46] G. von Essen, E. Lindsund, B. Cannon, J. Nedergaard, Adaptive facultative diet-induced thermogenesis in wild-type but not in UCP1-ablated mice, Am. J. Physiol.

Endocrinol. Metab. 313 (5) (2017) E515–E527.
[47] L.P. Kozak, Brown fat and the myth of diet-induced thermogenesis, Cell Metab. 11 (4) (2010) 263–267.
[48] S.W. Ma, D.O. Foster, B.E. Nadeau, J. Triandafillou, Absence of increased oxygen consumption in brown adipose tissue of rats exhibiting “cafeteria” diet-induced thermogenesis, Can. J. Physiol. Pharmacol. 66 (11) (1988) 1347–1354.
[49] J. Lee, J. Choi, S. Aja, S. Scafidi, M.J. Wolfgang, Loss of adipose fatty acid oxidation does not potentiate obesity at thermoneutrality, Cell Rep. 14 (6) (2016) 1308–1316.
[50] J. Nedergaard, B. Cannon, The changed metabolic world with human brown adipose tissue: therapeutic visions, Cell Metab. 11 (4) (2010) 268–272.
[51] A. Essadel, S. Bensaid Alaoui, R. Mssrouri, E. Mohammadine, S. Benamr, A. Taghy, et al., Hibernoma: a rare case of massive weight loss, Ann. Chir. 127 (3) (2002) 215–217.
[52] M.E. Lean, W.P. James, G. Jennings, P. Trayhurn, Brown adipose tissue in patients with phaeochromocytoma, Int. J. Obes. 10 (3) (1986) 219–227.
[53] M. Chondronikola, E. Volpi, E. Borsheim, C. Porter, P. Annamalai, S. Enerback, et al., Brown adipose tissue improves whole-body glucose homeostasis and insulin sensitivity in humans, Diabetes 63 (12) (2014) 4089–4099.
[54] M.J. Hanssen, J. Hoeks, B. Brans, A.A. van der Lans, G. Schaart, J.J. van den Driessche, et al., Short-term cold acclimation improves insulin sensitivity in patients with type 2 diabetes mellitus, Nat. Med. 21 (8) (2015) 863–865.
[55] J.M. Olsen, R.I. Csikasz, N. Dehvari, L. Lu, A. Sandstrom, A.I. Oberg, et al., beta3-Adrenergically induced glucose uptake in brown adipose tissue is independent of UCP1 presence or activity: mediation through the mTOR pathway, Mol. Metab. 6 (6) (2017) 611–619.
[56] A.M. Cypess, Y.C. Chen, C. Sze, K. Wang, J. English, O. Chan, et al., Cold but not sympathomimetics activates human brown adipose tissue in vivo, Proc. Natl. Acad. Sci. U. S. A. 109 (25) (2012) 10001–10005.
[57] A.M. Cypess, L.S. Weiner, C. Roberts-Toler, E. Franquet Elia, S.H. Kessler, P.A. Kahn, et al., Activation of human brown adipose tissue by a beta3-adrenergic receptor agonist, Cell Metab. 21 (1) (2015) 33–38.
[58] K.L. Marlatt, E. Ravussin, Brown adipose tissue: an update on recent findings, Curr. Obes. Rep. 6 (4) (2017) 389–396.